

# Radiative decay width of the $a_2(1320)^-$ meson

The SELEX Collaboration

V.V. Molchanov<sup>f,\*</sup>, G. Alkhazov<sup>k</sup>, A.G. Atamantchouk<sup>k,1</sup>,  
M.Y. Balatz<sup>h,1</sup>, N.F. Bondar<sup>k</sup>, D. Casey<sup>r</sup>, P.S. Cooper<sup>e</sup>,  
L.J. Dauwe<sup>q</sup>, G.V. Davidenko<sup>h</sup>, U. Dersch<sup>i,2</sup>,  
A.G. Dolgolenko<sup>h</sup>, G.B. Dzyubenko<sup>h</sup>, R. Edelstein<sup>c</sup>,  
L. Emediato<sup>t</sup>, A.M.F. Endler<sup>d</sup>, J. Engelfried<sup>m,e</sup>, I. Eschrich<sup>i,3</sup>,  
C.O. Escobar<sup>t,4</sup>, A.V. Evdokimov<sup>h</sup>, T. Ferbel<sup>r</sup>,  
I.S. Filimonov<sup>j,1</sup>, F.G. Garcia<sup>t,e</sup>, M. Gaspero<sup>s</sup>, I. Giller<sup>l</sup>,  
V.L. Golovtsov<sup>k</sup>, P. Gouffon<sup>t</sup>, E. Gülmez<sup>b</sup>, C. Hammer<sup>r</sup>,  
He Kangling<sup>g</sup>, M. Iori<sup>s</sup>, S.Y. Jun<sup>c</sup>, M. Kaya<sup>p</sup>, J. Kilmer<sup>e</sup>,  
V.T. Kim<sup>k</sup>, L.M. Kochenda<sup>k</sup>, I. Konorov<sup>i,5</sup>,  
A.P. Kozhevnikov<sup>f</sup>, A.G. Krivshich<sup>k</sup>, H. Krüger<sup>i,6</sup>,  
M.A. Kubantsev<sup>h</sup>, V.P. Kubarovsky<sup>f</sup>, A.I. Kulyavtsev<sup>c,e</sup>,  
N.P. Kuropatkin<sup>k,e</sup>, V.F. Kurshetsov<sup>f</sup>, A. Kushnirenko<sup>c</sup>,  
S. Kwan<sup>e</sup>, J. Lach<sup>e</sup>, A. Lamberto<sup>u</sup>, L.G. Landsberg<sup>f</sup>, I. Larin<sup>h</sup>,  
E.M. Leikin<sup>j</sup>, Li Yunshan<sup>g</sup>, M. Luksys<sup>n</sup>, T. Lungov<sup>t,7</sup>,  
V.P. Maleev<sup>k</sup>, D. Mao<sup>c,8</sup>, Mao Chensheng<sup>g</sup>, Mao Zhenlin<sup>g</sup>,  
P. Mathew<sup>c,9</sup>, M. Mattson<sup>c</sup>, V. Matveev<sup>h</sup>, E. McCliment<sup>p</sup>,  
M.A. Moinester<sup>l</sup>, A. Morelos<sup>m</sup>, V.A. Mukhin<sup>f</sup>,  
K.D. Nelson<sup>p,10</sup>, A.V. Nemitkin<sup>j</sup>, P.V. Neoustroev<sup>k</sup>,  
C. Newsom<sup>p</sup>, A.P. Nilov<sup>h</sup>, S.B. Nurushev<sup>f</sup>, A. Ocherashvili<sup>l,11</sup>,  
Y. Onel<sup>p</sup>, E. Ozel<sup>p</sup>, S. Ozkorucuklu<sup>p</sup>, A. Penzo<sup>u</sup>,  
S.V. Petrenko<sup>f</sup>, P. Pogodin<sup>p</sup>, M. Procario<sup>c,12</sup>, V.A. Prutskoi<sup>h</sup>,  
E. Ramberg<sup>e</sup>, G.F. Rappazzo<sup>u</sup>, B.V. Razmyslovich<sup>k</sup>,  
V.I. Rud<sup>j</sup>, J. Russ<sup>c</sup>, P. Schiavon<sup>u</sup>, J. Simon<sup>i,13</sup>, A.I. Sitnikov<sup>h</sup>,  
D. Skow<sup>e</sup>, P. Slattey<sup>r</sup>, V.J. Smith<sup>o</sup>, M. Srivastava<sup>t</sup>,  
V. Steiner<sup>l</sup>, V. Stepanov<sup>k</sup>, L. Stutte<sup>e</sup>, M. Svoiski<sup>k</sup>,  
N.K. Terentyev<sup>k,c</sup>, G.P. Thomas<sup>a</sup>, L.N. Uvarov<sup>k</sup>,  
A.N. Vasiliev<sup>f</sup>, D.V. Vavilov<sup>f</sup>, V.S. Verebryusov<sup>h</sup>,  
V.A. Victorov<sup>f</sup>, V.E. Vishnyakov<sup>h</sup>, A.A. Vorobyov<sup>k</sup>,  
K. Vorwalter<sup>i,14</sup>, J. You<sup>c,e</sup>, Zhao Wenheng<sup>g</sup>, Zheng Shuchen<sup>g</sup>,

Z.H. Zhu <sup>r</sup>, M. Zielinski <sup>r</sup>, R. Zukanovich-Funchal <sup>t</sup>

<sup>a</sup>*Ball State University, Muncie, IN 47306, U.S.A.*

<sup>b</sup>*Bogazici University, Bebek 80815 Istanbul, Turkey*

<sup>c</sup>*Carnegie-Mellon University, Pittsburgh, PA 15213, U.S.A.*

<sup>d</sup>*Centro Brasileiro de Pesquisas Físicas, Rio de Janeiro, Brazil*

<sup>e</sup>*Fermilab, Batavia, IL 60510, U.S.A.*

<sup>f</sup>*Institute for High Energy Physics, Protvino, Russia*

<sup>g</sup>*Institute of High Energy Physics, Beijing, P.R. China*

<sup>h</sup>*Institute of Theoretical and Experimental Physics, Moscow, Russia*

<sup>i</sup>*Max-Planck-Institut für Kernphysik, 69117 Heidelberg, Germany*

<sup>j</sup>*Moscow State University, Moscow, Russia*

<sup>k</sup>*Petersburg Nuclear Physics Institute, St. Petersburg, Russia*

<sup>l</sup>*Tel Aviv University, 69978 Ramat Aviv, Israel*

<sup>m</sup>*Universidad Autónoma de San Luis Potosí, San Luis Potosí, Mexico*

<sup>n</sup>*Universidade Federal da Paraíba, Paraíba, Brazil*

<sup>o</sup>*University of Bristol, Bristol BS8 1TL, United Kingdom*

<sup>p</sup>*University of Iowa, Iowa City, IA 52242, U.S.A.*

<sup>q</sup>*University of Michigan-Flint, Flint, MI 48502, U.S.A.*

<sup>r</sup>*University of Rochester, Rochester, NY 14627, U.S.A.*

<sup>s</sup>*University of Rome “La Sapienza” and INFN, Rome, Italy*

<sup>t</sup>*University of São Paulo, São Paulo, Brazil*

<sup>u</sup>*University of Trieste and INFN, Trieste, Italy*

---

## Abstract

Coherent  $\pi^+\pi^-\pi^-$  production in the interactions of a beam of 600 GeV  $\pi^-$  mesons with C, Cu and Pb nuclei has been studied with the SELEX facility (Experiment E781 at Fermilab). The  $a_2(1320)$  meson signal has been detected in the Coulomb (low  $q^2$ ) region. The Primakoff formalism used to extract radiative decay width of this meson yields  $\Gamma = 284 \pm 25 \pm 25$  keV, which is the most precise measurement to date.

*Key words:* Radiative decay, Primakoff effect,  $a_2(1320)$

*PACS:* 13.40.Hq, 13.60.Le, 14.40.Cs

---

## 1 Introduction

Radiative decays of mesons and baryons, as well as other electromagnetic processes, are important tools for studying internal structure of these particles and for testing unitary symmetry schemes and quark models of hadrons. Such processes, which are governed by interactions of real and virtual photons with electric charges of quark fields, make it possible to obtain unique information about the quark content of hadrons and about certain phenomenological parameters of hadrons (magnetic and electric transition moments, form factors, polarizabilities, etc). The underlying processes are simpler to analyze than purely hadronic phenomena, and can play an important role in testing chiral, bag, string and lattice models of hadrons.

Direct observation and study of rare radiative decays of hadrons of the type  $a \rightarrow h + \gamma$  is often very difficult to carry out because of high background from  $a \rightarrow h + \pi^0(\eta)$ ,  $\pi^0(\eta) \rightarrow 2\gamma$  decays, with one lost photon, and other hadronic processes with  $\pi^0(\eta)$  production. An alternative way to investigate such decays in coherent production in the Coulomb field of atomic nuclei was proposed initially by Primakoff, Pomeranchuk and Shmushkevich [1, 2]:

$$h + (A, Z) \rightarrow a + (A, Z) \quad (1)$$

The cross section for such reactions (which is usually referred to as Primakoff production) is proportional to the radiative decay width  $\Gamma(a \rightarrow h + \gamma)$ . It follows that by measuring the absolute cross section of the Coulomb contribution

---

\* Corresponding author.

*Email address:* molchanov@mx.ihep.su (V.V. Molchanov).

<sup>1</sup> deceased

<sup>2</sup> Present address: Infinion, München, Germany

<sup>3</sup> Now at Imperial College, London SW7 2BZ, U.K.

<sup>4</sup> Now at Instituto de Física da Universidade Estadual de Campinas, UNICAMP, SP, Brazil

<sup>5</sup> Now at Physik-Department, Technische Universität München, 85748 Garching, Germany

<sup>6</sup> Present address: The Boston Consulting Group, München, Germany

<sup>7</sup> Now at Instituto de Física Teórica da Universidade Estadual Paulista, São Paulo, Brazil

<sup>8</sup> Present address: Lucent Technologies, Naperville, IL

<sup>9</sup> Present address: SPSS Inc., Chicago, IL

<sup>10</sup> Now at University of Alabama at Birmingham, Birmingham, AL 35294

<sup>11</sup> Present address: Imadent Ltd., Rehovot 76702, Israel

<sup>12</sup> Present address: DOE, Germantown, MD

<sup>13</sup> Present address: Siemens Medizintechnik, Erlangen, Germany

<sup>14</sup> Present address: Deutsche Bank AG, Eschborn, Germany



This was singled out with the help of a special exclusive trigger. This trigger used scintillation counters to define beam time and to suppress interactions upstream of the target. Pulse height in the interaction counters was used to select events with exactly three charged tracks downstream of the target. The trigger hodoscope, which was located after two analyzing magnets, also required three charged tracks. Finally, to reduce the background trigger rate to an acceptable level, the aperture was limited by veto counters, which had little effect on efficiency for Reaction (3). A segmented target with 2 Cu and 3 C foils, each separated by 1.5 cm, was used for most of the data taking. A thin Pb target, which is important for the study of Coulomb production, was used only during brief periods of running because of the deleterious impact on charm measurements.

Only part of the SELEX facility was needed for the study of Reaction (3). The beam transition-radiation detector provided reliable separation of  $\pi^-$  from  $\Sigma^-$ . Silicon strip detectors (most of which had  $4\text{ }\mu\text{m}$  transverse position resolution) measured parameters of the beam and secondary tracks in the target region. After deflection by analyzing magnets, tracks were measured in 14 planes of 2 mm proportional wire chambers. The absolute momentum scale was calibrated using the  $K_S^0$  decays. Three-pion mass resolution in the  $a_2(1320)$  region was 14 MeV. A special on-line filter was used to reduce the number of exclusive events written to tape. Originally, this selected events that had at least one secondary reconstructed track, but it was modified subsequently to require at least two segments after the analyzing magnets. Very loose criteria were imposed on the number of hits in the tracking detectors to control processing time. All these requirements were not very restrictive, and are expected to have only minor effect on the process of interest.

### 3 Data analysis

Events for Reaction (3) were selected by requiring a reconstructed beam track and three charged tracks in the final state. These tracks were required to form a good vertex in the vicinity of one of the targets. The beam particle had to be identified as a pion by the beam TRD. However, there was no such requirement for the produced particles. To suppress inclusive ( $\pi^+\pi^-\pi^- + X$ ) background, the energy sum of the observed particles was required to be within  $\pm 17.5\text{ GeV}$  of the beam energy. For further suppression of these events, the most upstream photon detector was used as a guard system, requiring that any registered energy be less than 2 GeV. The number of events selected for Reaction (3) for different targets, and other information of interest, is summarized in Table 1.

Most of the ensuing analysis will be described using the data from the copper target. The distribution in the square of the transverse momentum ( $p_T^2$ ) of the

$3\pi$ -system in Reaction (3) is shown in Fig. 1. This distribution can be fitted by the sum of two falling exponentials, one with slope parameter  $b_1 \approx 180 \text{ GeV}^{-2}$ , which is characteristic of coherent diffractive production on a copper nucleus, and the other with a slope parameter  $b_2 \sim 1500 \text{ GeV}^{-2}$ , which is consistent with the estimation for Coulomb production folded in with the experimental resolution in transverse momentum. Data for C and Pb targets exhibit similar behavior (not shown), which establishes the presence of Coulomb production in Reaction (3) for all three targets.

Two  $p_T^2$  regions are defined for extracting the mass distribution for the Coulomb production process, as shown in Fig. 1. The first one ( $p_T^2 < 0.001 \text{ GeV}^2$ ) contains most of the Coulomb contribution, the second one ( $0.0015 < p_T^2 < 0.0035 \text{ GeV}^2$ ) has very little of it. But even the first region is dominated by diffractive production. The mass spectra  $M(3\pi)$  for these two regions are presented in Fig. 2. Using results of the fit to Fig. 1, the mass distribution for events in the second  $p_T^2$  region was normalized to the expected number of diffractive events in the first region. Then, the mass distribution from the second region was subtracted from the distribution for the first  $p_T^2$  region. This type of background subtraction assumes that the coherent nuclear background at smallest  $p_T$  is similar to that at the larger  $p_T$  values. The resulting mass spectrum is shown in Fig. 3. The  $a_2(1320)$  signal stands out clearly. Similar distributions for C and Pb targets are shown in Figs. 4 and 5. While the observed  $a_2$  signal is dominated by the electromagnetic production mechanism, there can be contributions to  $a_2$  production from strong interactions (e.g., via  $f_2$  exchange) and interference with other mechanisms of  $3\pi$  production (e.g., from  $a_1(1260)$  Primakoff production). Corrections for such effects, and the consequent uncertainties, will be discussed shortly below.

The differential cross section for Coulomb production of a broad resonance in a pion beam is given by the expression [8, 9, 10, 11]:

$$\frac{d\sigma}{dM dq^2} = 16\alpha Z^2 (2J + 1) \left( \frac{M}{M^2 - m_\pi^2} \right)^3 \frac{m_0^2 \Gamma(\pi\gamma) \Gamma(\text{final})}{(M^2 - m_0^2)^2 + m_0^2 \Gamma(\text{all})^2} \frac{q^2 - q_{\min}^2}{q^4} |F(q^2)|^2 \quad (4)$$

where  $\alpha$  is the fine structure constant,  $Z$  is the charge of the nucleus,  $J$  and  $m_0$  are spin and mass of the produced resonance,  $M$  is the effective mass of the produced system, the  $\Gamma$  are the decay widths for the corresponding modes,  $q^2$  is the square of the momentum transfer, and  $q_{\min}^2$  is its minimal value. At high beam momentum

$$q_{\min}^2 \approx \frac{(M^2 - m_\pi^2)^2}{4P_{\text{beam}}^2} \quad (5)$$

At our beam energy,  $q_{\min}^2$  is very small, and is  $\approx 2 \cdot 10^{-6} \text{ GeV}^2$  at the  $a_2$  mass. Consequently,  $q^2 \approx q_{\min}^2 + p_T^2 \approx p_T^2$ .

The Coulomb form factor  $F(q^2)$  in Eq. (4) accounts for the nuclear charge distribution, initial and final state absorption, as well as the Coulomb phase. It was calculated in the framework of the optical model described in Ref. [12]. This model requires knowledge of the total pion-nucleon cross section  $\sigma$ , and the ratio of real to imaginary parts of the forward scattering amplitude  $\rho'$ , at the appropriate beam energy. We used the cross section  $\sigma = 26.6$  mb determined in the SELEX experiment, and the extrapolated value of  $\rho' = 0.12$  [13]. The impact of  $F(q^2)$  at these energies is minimal.

The  $a_2$  final state was taken to be  $\rho\pi$ , and the total  $a_2$  width was parametrized as:

$$\Gamma = \Gamma_0 \frac{m_0}{M} \frac{k}{k_0} \frac{B_L(kR)}{B_L(k_0R)}, \quad (6)$$

where the  $k$  and  $k_0$  are center of mass momenta of  $a_2$  decays, off and on resonance, into the corresponding final states. The  $B_L$  are Blatt-Weisskopf centrifugal barrier factors, as given by von Hippel and Quigg [14]. The range of interactions  $R$  was taken as 1 fm;  $L$  is the orbital momentum and is equal to 2 for both  $\pi\gamma$  and  $\rho\pi$  decay modes.

To extract the radiative width  $\Gamma(a_2 \rightarrow \pi\gamma)$  from the Coulomb production of the  $a_2(1320)$  meson given by Eq. (4), requires an absolute normalization of the cross section. This means taking into account luminosity of the exposure and efficiency, which includes trigger, acceptance, reconstruction, as well as effects of transverse momentum resolution. The most difficult and uncertain procedure arises from the evaluation of the trigger performance. This is because of accidental veto rates, uncertainties in the discrimination of analog amplitudes, and other factors that varied during the run. That is why we chose to normalize the measurement to the three-pion diffractive production process, which dominates Reaction (3) in the region of  $q^2 \lesssim 0.4A^{-2/3} \text{ GeV}^2$ . As far as the trigger is concerned, both Coulomb and diffractive production have the same kinematics, thus, in such an analysis, all trigger and luminosity uncertainties cancel.

Our preliminary result [5] relied on a normalization to the diffractive cross sections measured by the E272 experiment [15]. But these data were obtained under different experimental conditions ( $\pi^+$  beam with an energy of 200 GeV) and had only limited ( $\sim 15\%$ ) precision. Also, we felt it important to avoid any correlation between our result for the  $a_2(1320)$  radiative decay width and that of the previous E272 measurement [16]. Thus, we chose to obtain an independent value for the diffractive three-pion cross section in the SELEX experiment, and normalized our result to the number of events under the first diffractive exponential of the  $p_{\text{T}}^2$  distribution, as described below.

SELEX had significant periods of running when all the three targets were employed simultaneously and the trigger did not distinguish between these targets. Thus differences in detection efficiency of Primakoff  $a_2$  and diffractive  $3\pi$  productions on different targets could be described reliably by MC simulations. Consequently, to obtain a normalization it was sufficient to measure the diffractive three-pion cross section on any of the three target nuclei.

To obtain an absolute normalization, we used special runs with a so-called “beam” trigger. This trigger employed scintillation counters to define beam particles and to reject halo, and used no information from detectors downstream of the targets. Thus, it selected a completely unbiased set of interactions. The incident flux was simply the number of reconstructed beam tracks. The three-pion mass was confined to  $0.8 < M(3\pi) < 1.5$  GeV, which contains most of the statistics, and for which the acceptance calculation (to be described later) is very reliable. Two exposures were analyzed with the beam trigger. In each, the largest samples (slightly more than a 1000 diffractive events) were collected with the carbon target, which became the natural choice for normalization. A carbon nucleus is also preferable because it is small, and therefore diffractive events do not display an irregular dependence on  $p_T^2$  (e.g., there is no large second diffractive maximum), which could produce additional systematic uncertainties.

The first carbon data sample included short calibration runs taken at least once a day under standard experimental conditions. These indicated that track reconstruction efficiency depended on beam intensity. An extrapolation to zero rate provided the result:  $\sigma_{\text{diff}}^{(1)} = 2.39 \pm 0.14$  mb for the cross section defined above. The second data set had special stand-alone runs used to measure total cross sections with SELEX [13]. These runs were characterized by low beam intensity ( $\lesssim 10$  kHz), use of special targets, and absence of field in the first spectrometer magnet. The latter led to somewhat higher acceptance, but worse reconstruction efficiency and momentum resolution. The measured value of the diffractive cross section in this data set was  $\sigma_{\text{diff}}^{(2)} = 2.67 \pm 0.10$  mb.

Since the experimental conditions in these independent data sets were different, it is reasonable to expect that systematic uncertainties were uncorrelated. The two measurements were therefore averaged. Because the  $\chi^2$  for the two was 2.6 rather than unity, we followed the usual PDG procedure of scaling the error by a factor of  $\sqrt{\chi^2}$ . Consequently, the final value used for the normalization on carbon is  $\langle \sigma_{\text{diff}} \rangle = 2.57 \pm 0.13$  mb. This result was extrapolated via MC to Primakoff production on all the targets.

Acceptance and reconstruction efficiencies for all processes were calculated using a GEANT-based Monte Carlo program [17]. As expected, the efficiency was independent of the  $q^2$  for the range relevant to this analysis ( $q^2 \lesssim 0.1$  GeV<sup>2</sup>). For Primakoff  $a_2$  production, the efficiency was calculated as a function of

mass, with decay kinematics simulated according to a  $\rho\pi$  in a  $2^+D1^+$  partial wave (where  $J^PLM^\eta$  corresponds to standard notation [18], with  $J^P$  being spin and parity of the produced system,  $L$  the relative orbital momentum between the  $\rho$  and  $\pi$ , and  $M^\eta$  the spin projection and naturality). For diffractive three-pion production kinematics, we used  $\rho\pi$  in  $1^+S0^+$  wave, which is expected to be dominant [19, 20]. The mass was restricted to  $0.8 < M_{3\pi} < 1.5$  GeV, because there is evidence of additional structure (presumably  $\pi_2(1670)$ ) at higher mass values. The shape of the  $\rho$ -meson was parametrized using Eq. (6). Comparison of observed and simulated angular and mass distributions showed good agreement, and thus supported the assumption about the dominance of the described production mechanism.

To determine the transverse momentum resolution we studied decays of  $\Xi^-$ , present in the beam. We had about 6800  $\Xi^- \rightarrow \Lambda\pi^-$ ,  $\Lambda \rightarrow p\pi^-$  decays, with both vertices lying within the target region. These events are topologically similar to those of Reaction (3), and correspond to no momentum transfer ( $p_T = 0$ ). Consequently, the measured momentum transfer gives the resolution. Comparison of measured values with MC showed that the transverse momentum resolution is different for the two transverse  $X$  and  $Y$  projections, both in data and MC, and that the resolution in the MC is better than in the data. This can be attributed to the idealization of geometry in the MC, and insufficient detail used in the simulation of detector response and noise. The difference in quadrature in the resolution between data and MC  $\sqrt{\sigma_{\text{data}}^2 - \sigma_{\text{MC}}^2}$  was found to be  $\approx 5$  MeV. This was used to correct the MC resolutions for  $a_2$  production, which, in general, depended on the data set, target and transverse direction. The final values vary from 16.2 to 19.3 MeV, and have relative uncertainty of  $\approx 2\%$ .

To obtain the expected shape of the  $a_2(1320)$  signal, Eq. (4) for Coulomb production was multiplied by efficiency, convoluted with the  $p_T$ -resolution, and integrated over the relevant region of  $p_T^2$ . To check the stability of the result, we varied the regions of  $p_T^2$  (14 combinations were used) and employed two different fitting procedures. In the first procedure, the subtracted mass distribution, such as the one shown in Fig. 3, was fitted with the sum of a resonance and a smooth background. In the second procedure, we fitted the mass distribution in the first region of  $p_T^2$  (open histogram in Fig. 2). To describe background, we used the distribution from the second (higher)  $p_T^2$  region (shaded histogram in Fig. 2), multiplied by a linear function of mass ( $a + bM$ ) to allow for small changes of shape in the mass spectrum. Results for different  $p_T^2$  regions and both fitting procedures were similar. They were used to calculate the average and to estimate statistical and systematical uncertainties.

The extracted radiative width does not depend strongly on the form assumed for the shape of the  $a_2$  resonance. This is because the same parametrization

must be used both in fitting the experimental data and in the expression for the Coulomb production cross section. In contrast, the total number of  $a_2$  events depends more strongly on the parametrization because of the relatively large resonance width. While this number is not used in the analysis (radiative width is determined directly from the fit), it provides a measure of the statistical accuracy. To reduce the dependence on parametrization, it is customary to count events in a limited mass region. Such numbers for each target are shown in Table 1.

When determining the mass and full width of the  $a_2$  from the fit, we find that they are close to the world average, while corresponding uncertainties ( $\sigma(M) \approx 6$  MeV and  $\sigma(\Gamma) \approx 20$  MeV) are much larger than the world average values [21]. We consequently fix the mass and width in the fit to their known PDG values. This has only a small impact on the extracted radiative width.

The  $a_2$  signal can be affected by interference with other  $3\pi$  Coulomb production processes. When integrated over the phase space, such interference effects are expected to be small due to large acceptance of the SELEX apparatus. One particular case of interest is Primakoff production of the  $a_1(1260)$  meson, where the dominant decay mode is also  $\rho\pi$  (it is the only meson close in mass to  $a_2$  and capable of decaying to  $\rho\pi$  and  $\pi^-\gamma$ ). Properties of this meson are not well known. The only measurement of its radiative width to  $\pi\gamma$  is  $640 \pm 246$  keV [25]. PDG estimation of the full width is 250–600 MeV. Using central values for both widths, root mean square value of interference effect on the measured  $a_2$  radiative width was estimated to be  $\approx 5\%$ . However, data on charge-exchange photoproduction [26], where no evidence of the  $a_1$  was found, while a clear  $a_2$  signal was observed, suggest either an extremely large  $a_1(1260)$  total width or small radiative width to  $\pi\gamma$ . Both possibilities decrease the magnitude of any interference effects. Given the small value of the described effect, and significant uncertainties in the properties of the  $a_1$  meson, we do not include this in the systematic uncertainty on the extracted width.

Because our fitting procedure ignores strong production of the  $a_2(1320)$  meson, the results of the fit must be corrected for this effect. It is impossible to correct for interference of the two amplitudes because the phase difference is not known. This contributes to a systematic uncertainty of  $\approx 4.5\%$  in the analysis. To describe strong production, we used the model developed in Ref. [12]. It uses a normalization factor for the  $a_2$  production on a single nucleon  $C_S$ , which must be extrapolated to our energy of 600 GeV. Production of the  $a_2$  meson has been measured on protons up to an energy of 94 GeV (see Ref. [22, 23] and references therein) and on nuclei at an energy of 23 GeV [24]. We used value  $C_S = 1.0 \pm 0.5$  mb/GeV<sup>4</sup>, a large error being assigned to account for the uncertainty in extrapolation. Corrections were applied for each combination of  $p_T^2$  regions, and their net effect on the measured radiative width was estimated

as  $\approx 3\%$ .

The corrected results of the fit for each target, with their statistical uncertainties, are shown in Table 1. Since most of the factors that contribute to

Parameter	C	Cu	Pb
Total number of $3\pi$ events	$2.55 \cdot 10^6$	$1.82 \cdot 10^6$	$0.55 \cdot 10^6$
Approximate number of $a_2$ events*	1100	3700	2300
Radiative width [keV]	350	270	291
Statistical uncertainty [keV]	121	38	36

\* This is defined as the number of resonance events in 1.2–1.4 GeV mass region in the fits shown in Figs. 3–5. This differs from the preliminary results in Ref. [5].

Table 1

Characteristics of data on Coulomb  $a_2(1320)$  production on different targets.

systematic uncertainty are at least partially correlated for different targets, the results were averaged over three targets using only the statistical errors. Systematic uncertainties include absolute normalization (5%), correction for strong  $a_2$  production (1.5%), interference with strong  $a_2$  production (4.5%), transverse momentum resolution (1.8%), accuracy in  $F(q^2)$  calculation (1%), and uncertainties in the PDG parameters of the  $a_2(1320)$  resonance mass (0.35%), width (3.4%), and branching to  $\rho\pi$ <sup>15</sup> (3.8%). All sources were added in quadrature, and the final combined result is:

$$\Gamma[a_2(1320)^- \rightarrow \pi^- \gamma] = 284 \pm 25 \pm 25 \text{ keV} \quad (7)$$

This is the best measurement to date (total relative uncertainty of 12.5%). Comparison with the previous direct measurement [16] in the  $a_2^+ \rightarrow \eta\pi^+$  and  $K_S^0 K^+$  decay modes, and with theoretical predictions, is given in Table 2.

### Acknowledgements

The authors are indebted to the staff of the Fermi National Accelerator Laboratory, and for invaluable technical support from the staffs of collaborating institutions. This project was supported in part by Bundesministerium für Bildung, Wissenschaft, Forschung und Technologie, Consejo Nacional de Ciencia y Tecnología (CONACyT), Conselho Nacional de Desenvolvimento Científico e Tecnológico, Fondo de Apoyo a la Investigación (UASLP), Fundação de

<sup>15</sup> In fact, the relevant branching is  $a_2 \rightarrow 3\pi$ . Possible non- $\rho\pi$  contribution to this decay would affect angular distributions and the resonance shape, but the effect of this on the measured radiative width is negligible.

	$\Gamma [a_2(1320) \rightarrow \pi\gamma], \text{ keV}$
<i>Direct experimental measurements</i>	
SELEX collboration (this experiment)	$284 \pm 25 \pm 25$
E272 collaboration [16]	$295 \pm 60$
<i>Theoretical predictions</i>	
VDM model [27]	348
relativistic quark model [28]	324
covariant oscillator quark model [29]	235

Table 2

Experimental measurements of  $\Gamma [a_2(1320) \rightarrow \pi\gamma]$ , and comparison with theoretical predictions.

Amparo à Pesquisa do Estado de São Paulo (FAPESP), the Israel Science Foundation founded by the Israel Academy of Sciences and Humanities, Istituto Nazionale di Fisica Nucleare (INFN), the International Science Foundation (ISF), the National Science Foundation (Phy #9602178), NATO (grant CR6.941058-1360/94), the Russian Academy of Science, the Russian Ministry of Science and Technology, the Turkish Scientific and Technological Research Board (TÜBİTAK), the U.S. Department of Energy (DOE grant DE-FG02-91ER40664 and DOE contract number DE-AC02-76CHO3000), and the U.S.-Israel Binational Science Foundation (BSF).

The authors are also grateful to Prof. B. Povh for support of the work connected with diffractive three-pion production.

## References

- [1] H. Primakoff, Phys. Rev. 81 (1951) 899.
- [2] I.Ya. Pomeranchuk and I.M. Shmushkevich, Nucl. Phys. 23 (1961) 452.
- [3] T. Ferbel, Acta Physica Polonica B12 (1981) 1129.  
M. Zielinski, Acta Physica Polonica B18 (1987) 455.  
L. Landsberg, Physics of Atomic Nuclei 63 (2000) 1.
- [4] E.N. May et al., Phys. Rev. D16 (1977) 1983.
- [5] V. Kubarovsky, Radiative width of the  $a_2$  meson, in *Proceedings of the 29th International Conference on High Energy Physics*, pages 1296–1299, 1999, hep-ex/9901014.
- [6] V. Smith, in *Proceedings of the 7th International Conference on Hadron Spectroscopy (HADRONS-97)*, edited by S.-U. Chung and H. Willutzki, page 627, 1997.
- [7] J. Russ, Nucl. Phys. A585 (1995) 39.

- J. Russ et al., in *Proceedings of the 29th International Conference on High Energy Physics*, page 1259, 1999, hep-ex/9812031.
- [8] A. Halprin, C.M. Andersen and H. Primakoff, Phys. Rev. 152 (1966) 1295.
  - [9] G. Fäldt, Nucl. Phys. B43 (1972) 591.
  - [10] J.D. Jackson, Nuovo Cim. 34 (1964) 1644.
  - [11] J. Huston et al., Phys. Rev. D33 (1986) 3199.
  - [12] C. Bemporad et al., Nucl. Phys. B51 (1973) 1.
  - [13] U. Dersch et al., Nucl. Phys. B579 (2000) 277.
  - [14] F. von Hippel and C. Quigg, Phys. Rev. D5 (1972) 624.
  - [15] M. Zielinski et al., Z. Phys. C16 (1983) 197.
  - [16] S. Cihangir et al., Phys. Lett. B117 (1982) 119.
  - [17] G. Davidenko et al., GE781: a Monte Carlo package for fixed target experiments, in *Proceedings of the International Conference on Computing in High Energy Physics'95*, page 832, September 1995.
  - [18] J. Hansen et al., Nucl. Phys. B81 (1974) 403.
  - [19] M. Zielinski et al., Phys. Rev. D30 (1984) 1855.
  - [20] D. Amelin et al., Phys. Lett. B356 (1995) 595.
  - [21] D.E. Groom et al., Eur. Phys. J. C15 (2000) 1.
  - [22] C. Daum et al., Phys. Lett. 89B (1980) 276.
  - [23] W.E. Cleland et al., Nucl. Phys. B208 (1982) 228.
  - [24] T. Roberts et al., Phys. Rev. D18 (1978) 59.
  - [25] M. Zielinski et al., Phys. Rev. Lett. 52 (1984) 1195.
  - [26] G. Condo et al., Phys. Rev. D48 (1993) 3045.
  - [27] J. Babcock and J.L. Rosner, Phys. Rev. D14 (1976) 1286.
  - [28] I.G. Aznauryan and K.A. Oganessian, Sov. J. Nucl. Phys. 47 (1988) 1097.
  - [29] S. Ishida, K. Yamada and M. Oda, Phys. Rev. D40 (1989) 1497.

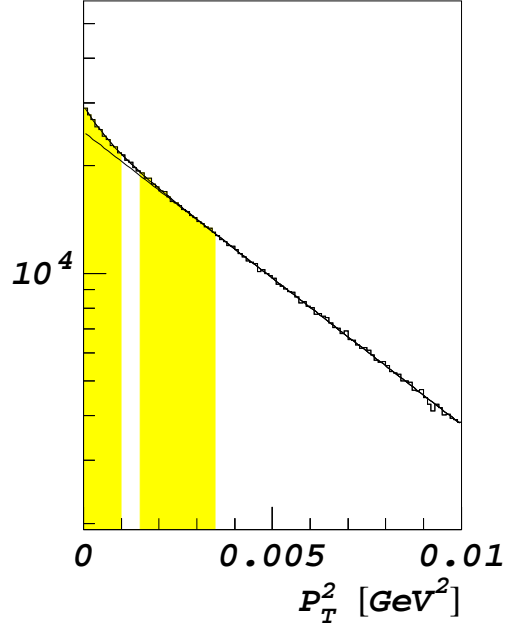


Fig. 1. Transverse momentum distribution for Reaction (3) on a Cu target.

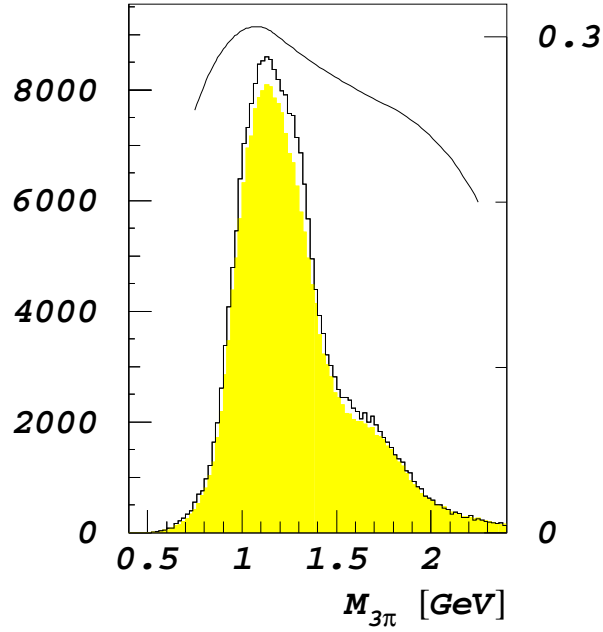


Fig. 2. Mass distribution for events with  $p_T^2 < 0.001 \text{ GeV}^2$  (histogram) and  $0.0015 < p_T^2 < 0.0035 \text{ GeV}^2$ , after normalization for background subtraction (shaded) according to Fig. 1. The curve shows the efficiency for observing a  $\rho\pi$  in a  $1^+S0^+$  wave, which is dominant in the shown mass spectrum.

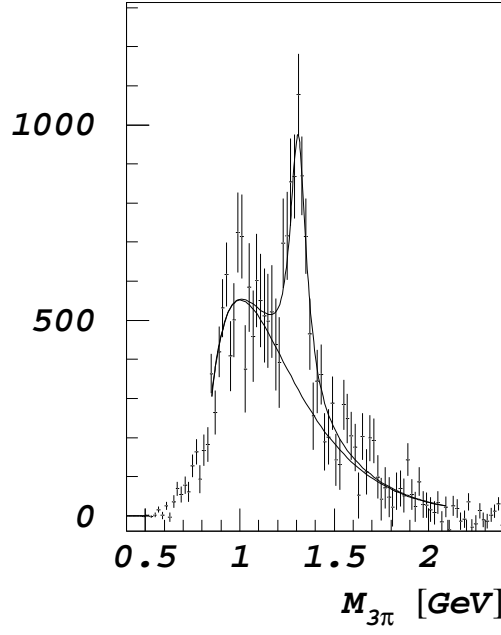


Fig. 3.  $M_{3\pi}$  mass distribution for the Cu target after subtraction of diffractive background. The curve shows fit with a sum of pure Coulomb contribution and smooth background.

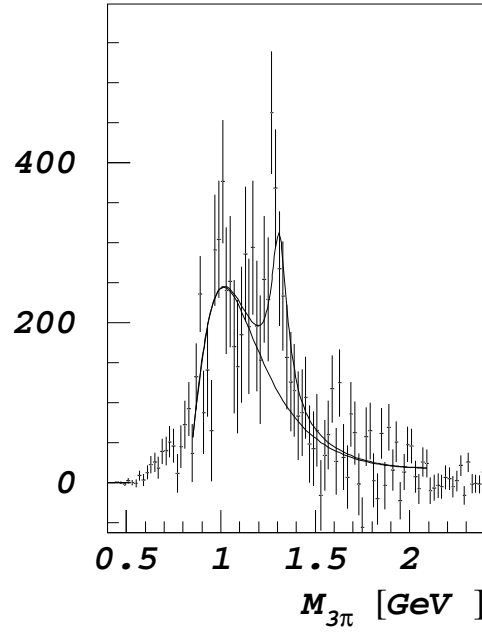


Fig. 4. The same as Fig. 3, but for C target.

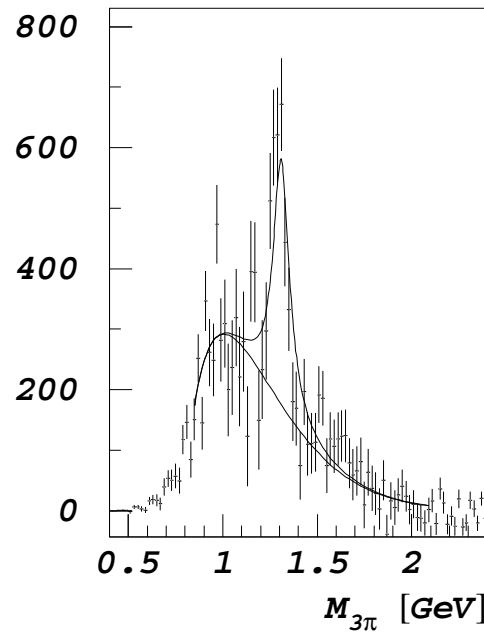


Fig. 5. The same as Fig. 3, but for Pb target.